



Applying Two-Dimensional Piecewise-Polynomial Basis for Medical Image Processing

H.N.Zaynidinov¹, I.Yusupov², J.U.Juraev³, J.S. Jabbarov⁴.

¹Tashkent university of Information technologies named after Muhammad al-Khwarizmi, Uzbekistan, tet2001@rambler.ru

²Tashkent university of Information technologies named after Muhammad al-Khwarizmi, Uzbekistan, ibrohimbek.211_10@mail.ru

³Samarkand state university, Uzbekistan, jurayevju@mail.ru

⁴Samarkand state university, Uzbekistan, jamoliddin.jabbarov@mail.ru

ABSTRACT

In this paper, determining the recovery coefficients outcome of digital processing of radiographic images by using two-dimensional piece-polynomial basis, image compression and algorithms have been developed that is quality imaging compared to the first image processing. We know that one of the main problem on image compression is to find and apply an effective method that allows each type of pixel to be displayed in a compact form. In order to solve this problem, two-dimensional piece-polynomial basis are used, and as a result, the compression and recovery coefficients of the image were determined.

Key words : two-dimensional Haar basis, one-dimensional Haar basis, digital image processing, recovery coefficients, Haar's fast transform algorithm.

1. INTRODUCTION

Traditional harmonic functions are widely used to build models of signals received from real objects. This is due to the fact that many signals received from real objects can be easily represented by a set of sinusoidal and cosine oscillations, for which the Fourier analysis tools are used. This results in transition from temporal to frequency functions. However, the representation of a time function by sinusoidal and cosine functions is only one of many representations. Any complete system of orthogonal functions can be applied to expand into series that correspond to the Fourier series[1]. Elementary functions, which are solutions to simple differential equations, are very widely used in practical engineering problems. Usually in the engineering literature, the term elementary is understood as generally simple functions of one or two variables, having a limited number of extrema, without breakpoints, with a limited slope within a given range of variation of the argument. They are used to build mathematical models of signals received from real objects.

2. ONE-DIMENSIONAL PIECE-POLYNOMIAL BASIS

Orthogonal systems of basis functions defined on the real

axis, for which there are also fast transformation algorithms, are widespread in technical applications. They can be divided into two classes:

- 1) Global basis functions - those whose values are not equal to zero on any subinterval [9]. This class includes Walsh functions [10], numeric, sawtooth;
- 2) Localized basis functions, nonzero values of which are specified on nested segments. Here are the examples for Haar [3] and Harmut functions[6].

Partitioning the real axis - usually binary - rational. In the future, we will mainly consider about the interval [0, 1] or [0, 1) and use the concept of a binary segment, which is obtained by dividing given interval into 2^p equal parts ($p = 1, 2, \dots$):

$$h_k = h_{pj} = \left[\frac{j}{2^{p-1}} \frac{j+1}{2^{p-1}} \right]; \quad (1)$$

where $j = 0, 1, \dots, 2^{p-1}$, $k = j + 2^{p-1}$

Examples of binary line segments are intervals

$$[0; 1); [1/2; 3/4], [3/8; 4/8] \text{ and etc.}$$

The length of the binary segment h_{pj} is

$$|h_{pj}| = \left| h_{pj}^+ \right| + \left| h_{pj}^- \right| = 2^{1-p};$$

Where h_{pj}^- , h_{pj}^+ are, respectively, its left and right halves and also represent binary segments:

$$h_{pj}^+ = \left[\frac{j-1}{2^{p-1}}; \frac{2j-1}{2^p} \right], \quad h_{pj}^- = \left[\frac{2j-1}{2^p}; \frac{j}{2^{p-1}} \right] \quad (2)$$

The system of unnormalized Haar functions in continuous form is defined [7]:

$$har_k(x) = har_{pj}(x) = \begin{cases} +1 & x \in h_{pj}^- \\ -1 & x \in h_{pj}^+ \\ 0 & x \in h_{pj} \end{cases} \quad (3)$$

It should be noted that $har_0(x) \equiv 1$

The number P is called the order of the Haar functions.

It is known that the Haar series [30]:

$$f(x) = \sum_{k=0}^{\infty} C_k \cdot har_k(x) \tag{4}$$

can provide both uniform (including uniform best) and root-mean-square approximation. It all depends on how the odds are calculated.

Specialists mostly pay attention for Haar and Harmut basis for two reasons:

1. Reducing the number of coefficients required for the approximation (with a given accuracy) in relation to the total number of binary segments.
2. Absence of “long” operations in expression (4). Only addition, subtraction and shift operations are used.

The disadvantage of Haar and Harmut rectangular orthogonal basis is the weak convergence of series in piecewise constant functions, i.e. the need to memorize several 100 coefficients for many functions in order to ensure errors of the order of 0.1%.

The search for methods to reduce the size of tables of coefficients, improve the "smoothness" indicators in an obvious way lead to systems of piecewise polynomial basis functions of a higher degree. Piecewise-linear basis functions (Schauder functions) are obtained most simply as a result of integration with a variable upper limit of orthogonal piecewise-constant Haar functions:

$$Shd_k(x) = 2^P \int_0^x har_k(r) dr \tag{5}$$

It should be considered that:

$$Shd_0^0(x) \equiv 1 \quad \text{and} \quad Shd_0^0(x) = x$$

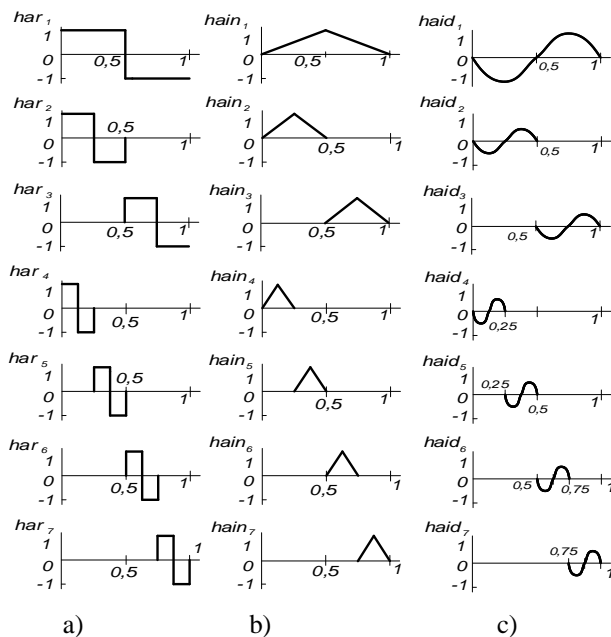


Figure 1: a) Piecewise-constants, b) Piecewise-linear c) Piecewise-quadratic Haar basis functions.

Often, in practical applications of series of piecewise linear functions in order to obtain the amplitudes of all basis

functions equal to one, it is convenient to operate with “normalized” systems:

$$\tilde{shd}_k(x) = 2^P \int_0^x har_k(r) dr \tag{6}$$

$$P = 0, 1, \dots; \quad k = 0, 1, 2, \dots$$

In Figure 1 a) the piecewise constant Haar functions are shown

b) Schauder functions c) piecewise parabolic Haar functions.

3. TWO-DIMENSIONAL POLYNOMIAL BASIS

The technique for constructing two-dimensional integral Haar bilinear basis functions can be based on the idea of integrating piecewise-planar orthogonal basis functions [1]. For example, two-dimensional Schauder functions can be plotted $Shd_{ij}(x,y) = Shd_i(x) * Shd_j(y)$ as a result of the operation of double integration:

$$Shd_{ij}(x,y) = \int_0^x \int_0^y har_i(\tau) har_j(\tau') d\tau d\tau' \tag{7}$$

The result is the so-called functions - "pagodas", the shape of one of which is shown in Figure 2a. The coefficients of discrete spectral transformations in bilinear basis are calculated using the so-called “diagonal” two-dimensional finite differences:

$$\Delta f_{ij} = f(x_{i+1}, y_{j+1}) - f(x_i, y_j) \tag{8}$$

These differences are the hypotenuses of vertical triangles, one of the cathetus of which is the heights of the pagodas (Figure 2a), and the other cathetus is the diagonal of an elementary area of size $h \times h$ on the plane (x, y) (Figure 2b).

Its length is indicated as Δ_{ij}

For two-dimensional bilinear basis, discrete transformation coefficients are determined by the formulas:

$$C_{kl} = \sum_i \sum_j \Delta f_{ij} har_k(x_i) har_l(x_j) \tag{9}$$

We form a system of basis functions depending on one of the arguments:

$$a_k(y) = \sum_j \Delta f_{ij} har_l(y) \tag{10}$$

Then we can write:

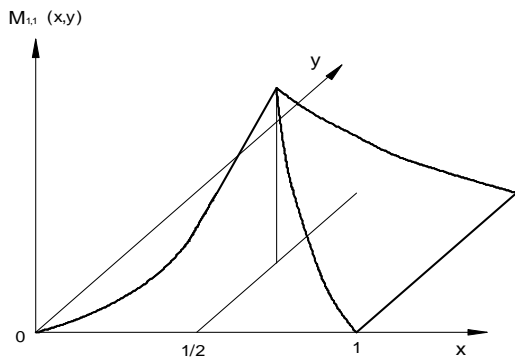
$$C_{kl} = \sum_i a_k(y) har_k(x) \tag{11}$$

Due to the real nature of the basis functions, the inverse two-dimensional discrete transformation is performed similarly [2]:

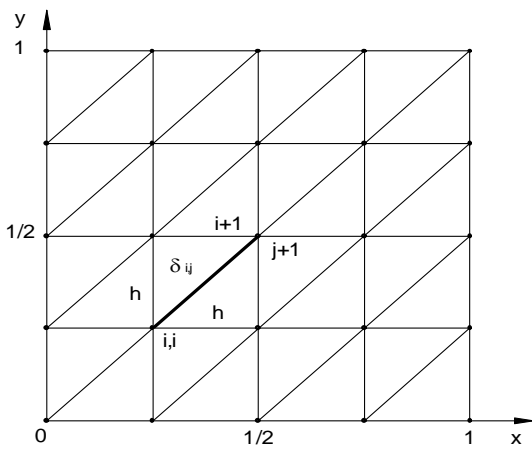
$$\Delta f_{ij} = 4^{-P} \sum_k \sum_l C_{kl} har_k(x) har_l(y) \tag{12}$$

$$\delta f_i(y) = \sum_l C_{kl} har_k(x) har_l(y)$$

$$\Delta f_{ij} = 4^{-p} \sum_k \delta f_i(y) \text{har}_k(x)$$



a) Two-dimensional M functions



b) Projection of diagonal differences

Figure 2: Two-dimensional M-functions and projection of diagonal differences

A system of piecewise-planar orthogonal Haar-like functions can be constructed on the basis of the theory of self-similar trees in a dynamic discrete space. The beginning of the process is the division of the unit square (Figure 3) into dyadic-rational regions, which are also squares, and groups of basis functions are built on these squares, taking the values +1, -1 or 0.

Arbitrary point (x, y) areas Ω ($0 \leq x, y < 1$) belongs to the binary square Q_{psr} , if the coordinates of this point belong to the corresponding binary segments $x \in h_{ps}^+$, $y \in h_{pr}^+$. Each square Q_{psr} contains four equal parts, which in turn are binary squares. Point (x, y) belongs to a dynamically decreasing square under the conditions [3]:

$$\begin{cases} (x, y) \in Q1_{psr}, & \text{if } x \in h_{ps}^+ \text{ and } y \in h_{pr}^+ \\ (x, y) \in Q2_{psr}, & \text{if } x \in h_{ps}^+ \text{ and } y \in h_{pr}^- \\ (x, y) \in Q3_{psr}, & \text{if } x \in h_{ps}^- \text{ and } y \in h_{pr}^+ \\ (x, y) \in Q4_{psr}, & \text{if } x \in h_{ps}^- \text{ and } y \in h_{pr}^- \end{cases}$$

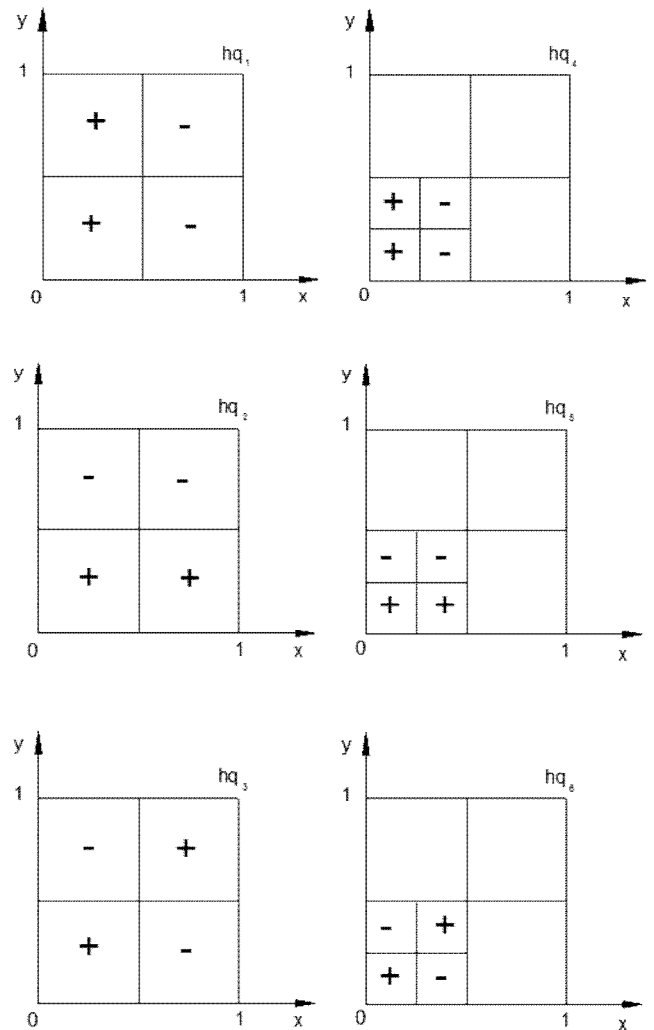


Figure 3: System of two-dimensional piecewise-plane functions

Thus, a recursive ordering is performed with the corresponding hierarchical numbering. On a square Q_{psr} three orthogonal functions are formed $Q_{psr} + 1$ or -1 with index $l = 1, 2$ and 3 :

$$\begin{aligned} hq_{psr1}(x, y) = hq_{ps}(x) &= \begin{cases} +1 \text{ at } x \in h_{ps}^+ \\ -1 \text{ at } x \in h_{ps}^- \end{cases} \\ hq_{psr2}(x, y) = hq_{pr}(y) &= \begin{cases} +1 \text{ at } y \in h_{pr}^+ \\ -1 \text{ at } y \in h_{pr}^- \end{cases} \\ hq_{psr3}(x, y) = hq_{pr}(y) &= \begin{cases} +1 \text{ at } y \in h_{pr}^+ \\ -1 \text{ at } x \in h_{pr}^- \end{cases} \end{aligned}$$

In a group of the same order p contains $3 * 4^{p-1}$ function[9].

4. TRANSFORMATION TWO-DIMENSIONAL PIECE WISE- POLYNOMIAL BASIS OF HAAR

For example, 2×2 given massive of two-dimensional monochrome images[3],

$$\left[x_{i,j} \right] \quad i = 1, \dots, 2^n ; \quad j = 1, \dots, 2^n \quad (13)$$

It can be expressed as a function of two variables $[0,1] \times [0,1]$, the part of which is defined in the unit field[8]. For a given two-variable function $f(s,t)$

$$f(s,t) = \sum_{i=1}^{2^n} \sum_{j=1}^{2^n} x_{i,j} H_{I_i \times I_j}(s,t) \quad (14)$$

Let the equality be fulfilled, here

$$I_i \times I_j = \left[\frac{i-1}{2^n}, \frac{i}{2^n} \right] \times \left[\frac{j-1}{2^n}, \frac{j}{2^n} \right] = \left\{ (s,t) : s \in \left[\frac{i-1}{2^n}, \frac{i}{2^n} \right], t \in \left[\frac{j-1}{2^n}, \frac{j}{2^n} \right] \right\}$$

and

$$H_{I_i \times I_j}(s,t) = \begin{cases} 1, & (s,t) \in I_i \times I_j \\ 0, & (s,t) \notin I_i \times I_j \end{cases} = H_{I_i}(s) H_{I_j}(t) = \frac{\phi_{n,i-1}(s)}{\sqrt{2^n}} \frac{\phi_{n,j-1}(t)}{\sqrt{2^n}} \quad (15)$$

The parameter s entered here is placed vertically and by substituting (3) into (2) we obtain the index i of the massive $x_{i,j}$ [8].

$$f(s,t) = \frac{1}{2^n} \sum_{i=1}^{2^n} \sum_{j=1}^{2^n} x_{i,j} \phi_{n,i-1}(s) \phi_{n,j-1}(t) = \frac{1}{2^n} \sum_{i=1}^{2^n} \left\{ \sum_{j=1}^{2^n} x_{i,j} \phi_{n,j-1}(t) \right\} \phi_{n,i-1}(s) = \frac{1}{2^n} \sum_{i=1}^{2^n} z_i(t) \phi_{n,i-1}(s) \quad (16)$$

here

$$z_i(t) = \sum_{j=1}^{2^n} x_{i,j} \phi_{n,j-1}(t) \quad (17)$$

For each one step (5) is similar to equation (3) and the first step of a one-dimensional QHT is performed [7]. We, we have a different form of equation for $z_i(t)$, $i=1,2,\dots,2^n$ (see formula 2)

$$z_i(t) = \sum_{j=0}^{2^{n-1}-1} a_{n-1,j}^i \phi_{n-1,j}(t) + \sum_{j=0}^{2^{n-1}-1} d_{n-1,j}^i \psi_{n-1,j}(t) \quad (18)$$

Now we replace (6) with (4) and form the following

$$f(s,t) = \frac{1}{2^n} \sum_{i=1}^{2^n} z_i(t) \phi_{n,i-1}(s) = \frac{1}{2^n} \sum_{i=1}^{2^n} \left(\sum_{j=0}^{2^{n-1}-1} a_{n-1,j}^i \phi_{n-1,j}(t) + \sum_{j=0}^{2^{n-1}-1} d_{n-1,j}^i \psi_{n-1,j}(t) \right) \phi_{n,i-1}(s) = \frac{1}{2^n} \left(\sum_{j=0}^{2^{n-1}-1} \left\{ \sum_{i=1}^{2^n} a_{n-1,j}^i \phi_{n,i-1}(s) \right\} \phi_{n-1,j}(t) + \sum_{j=0}^{2^{n-1}-1} \left\{ \sum_{i=1}^{2^n} d_{n-1,j}^i \psi_{n-1,j}(t) \right\} \phi_{n,i-1}(s) \right) = \frac{1}{2^n} \left(\sum_{j=0}^{2^{n-1}-1} \alpha_j(s) \phi_{n-1,j}(t) + \sum_{j=0}^{2^{n-1}-1} \beta_j(s) \psi_{n-1,j}(t) \right) \quad (19)$$

$$\begin{aligned} & + \sum_{j=0}^{2^n} d_{n-1,j}^i \psi_{n-1,j}(t) \Big) \phi_{n,i-1}(s) = \\ & = \frac{1}{2^n} \left(\sum_{j=0}^{2^{n-1}-1} \left\{ \sum_{i=1}^{2^n} a_{n-1,j}^i \phi_{n,i-1}(s) \right\} \phi_{n-1,j}(t) + \sum_{j=0}^{2^{n-1}-1} \left\{ \sum_{i=1}^{2^n} d_{n-1,j}^i \psi_{n-1,j}(t) \right\} \phi_{n,i-1}(s) \right) \\ & = \sum_{j=0}^{2^{n-1}-1} \alpha_j(s) \phi_{n-1,j}(t) + \sum_{j=0}^{2^{n-1}-1} \beta_j(s) \psi_{n-1,j}(t) \end{aligned} \quad (19)$$

Here

$$\alpha_j(s) = \sum_{i=0}^{2^n} a_{n-1,j}^i \phi_{n,i-1}(s) \quad \text{and} \quad \beta_j(s) = \sum_{i=1}^{2^n} d_{n-1,j}^i \psi_{n-1,i}(s)$$

for j α_j and β_j the expressions are constant and are similar to (3). One-dimensional QHT can be applied to it. By doing this, we get the following[13],

$$\begin{aligned} \alpha_j(t) &= \sum_{i=0}^{2^n} a_{n-1,j}^i \phi_{n,i-1}(s) = \sum_{i=0}^{2^{n-1}-1} \tilde{a}_{n-1,i}^j \phi_{n-1,i}(s) + \sum_{i=0}^{2^{n-1}-1} \tilde{d}_{n-1,i}^j \psi_{n-1,i}(s) \\ \beta_j(t) &= \sum_{i=0}^{2^n} d_{n-1,j}^i \psi_{n-1,i}(s) = \sum_{i=0}^{2^{n-1}-1} \tilde{a}_{n-1,i}^j \phi_{n-1,i}(s) + \sum_{i=0}^{2^{n-1}-1} \tilde{d}_{n-1,i}^j \psi_{n-1,i}(s) \end{aligned}$$

here

$$\begin{aligned} f(s,t) &= \frac{1}{2^n} \left(\sum_{i=1}^{2^{n-1}-1} \alpha_j(s) \phi_{n-1,j}(t) + \sum_{i=1}^{2^{n-1}-1} \beta_j(s) \psi_{n-1,j}(t) \right) = \\ &= \frac{1}{2^n} \left(\sum_{j=0}^{2^{n-1}-1} \left\{ \sum_{i=0}^{2^{n-1}-1} \tilde{a}_{n-1,i}^j \phi_{n-1,i}(s) + \sum_{i=0}^{2^{n-1}-1} \tilde{d}_{n-1,i}^j \psi_{n-1,i}(s) \right\} \phi_{n,j}(t) + \right. \end{aligned}$$

$$\begin{aligned}
 &+ \sum_{j=0}^{2^{n-1}-1} \left\{ \sum_{i=0}^{2^{n-1}-1} \tilde{a}_{n-1,i}^j \phi_{n-1,i}(s) + \right. \\
 &\left. + \sum_{i=0}^{2^{n-1}-1} \tilde{d}_{n-1,j}^i \psi_{n-1,i}(s) \right\} \psi_{n-1,j}(t)
 \end{aligned}$$

Considering the given equations, we get the following,

$$\begin{aligned}
 f(s,t) = & \sum_{i=0}^{2^{n-1}-1} \sum_{j=0}^{2^{n-1}-1} a_{i,j}^{n-1} \phi_{n-1,j}(t) \phi_{n-1,i}(s) + \\
 & + \sum_{i=0}^{2^{n-1}-1} \sum_{j=0}^{2^{n-1}-1} h_{i,j}^{n-1} \phi_{n-1,j}(t) \psi_{n-1,i}(s) + \\
 & + \sum_{i=0}^{2^{n-1}-1} \sum_{j=0}^{2^{n-1}-1} v_{i,j}^{n-1} \psi_{n-1,j}(t) \phi_{n-1,i}(s) + \\
 & + \sum_{i=0}^{2^{n-1}-1} \sum_{j=0}^{2^{n-1}-1} d_{i,j}^{n-1} \psi_{n-1,j}(t) \psi_{n-1,i}(s)
 \end{aligned} \tag{20}$$

here

$$\begin{aligned}
 a_{i,j}^{n-1} &= \frac{1}{2^n} \tilde{a}_{n-1,i}^j, & h_{i,j}^{n-1} &= \frac{1}{2^n} \tilde{d}_{n-1,i}^j, \\
 v_{i,j}^{n-1} &= \frac{1}{2^n} \tilde{a}_{n-1,i}^j, & d_{i,j}^{n-1} &= \frac{1}{2^n} \tilde{d}_{n-1,i}^j
 \end{aligned}$$

As a result, the functions are divided into the following functions [4], $\phi_{n-1,j}(t)\phi_{n-1,i}(s)$, $\phi_{n-1,j}(t)\psi_{n-1,i}(s)$, and

$$\psi_{n-1,j}(t)\phi_{n-1,i}(s), \psi_{n-1,j}(t)\psi_{n-1,i}(s)$$

Thus, the first phase of two-dimensional XM is continued by applying the first phase of one-dimensional QHT to each line of the image and then applying the first phase of one-dimensional QHT to each line of the masive .

The above (8) is two-dimensional piecewise- polynomial basis of Haar equation, which requires finding a large number of coefficients. The use of a long chain of coefficients and signal values allows to improve the quality of signal recovery[14]. Filtering of signals is performed using two types of filters, high frequency (HF) and low frequency (LF), as shown in Figure 1. As a result, the image is divided into four parts[4]: LFLF, LFHF, HFHF and HF. As you know, because the image is two-dimensional, filtering pixel values is done first by columns, then by rows. During the filtering process, the pixel color values are multiplied by the piecewise- polynomial basis of Haar coefficients and are the sum of the result. Thus, this conversion process continues until the last pixel of the image is etched[6].

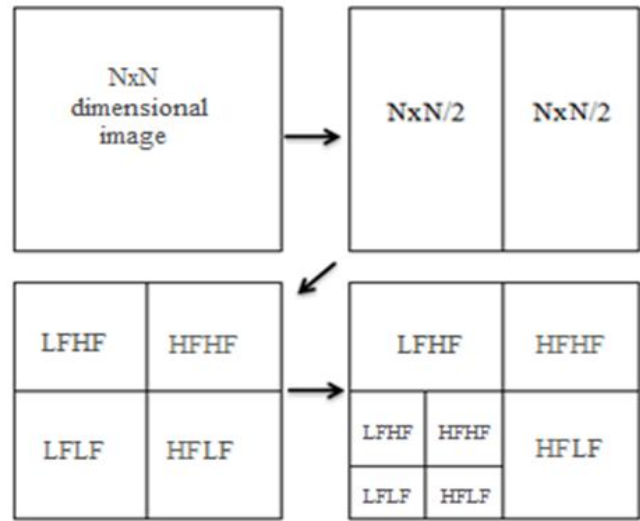


Figure 4: 1st and 2nd degree fragmentation scheme of images in two-dimensional piecewise- polynomial basis of Haar

Suppose we were given an X-ray of the head. C ++ Builder and Matlab programs based on the model shown in (8) were used to improve the quality of the stain in that image [11]. The following results were obtained after Level 1 fragmentation and Level 2 fragmentation (Figure 4, Figure 5)[10].

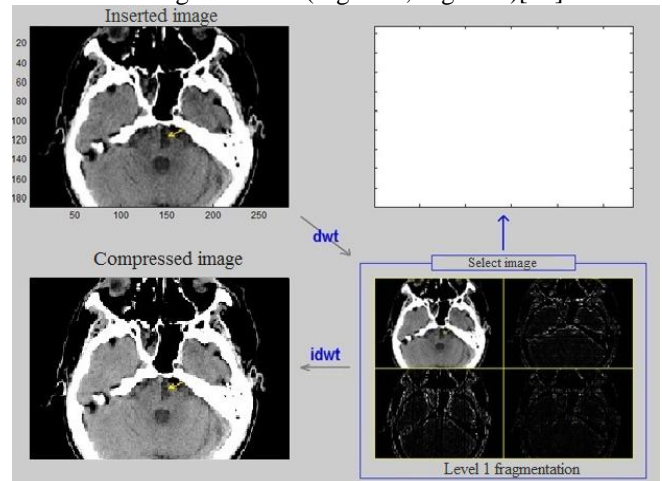


Figure 5: 1st degree fragmentation in two-dimensional piecewise- polynomial basis of Haar.

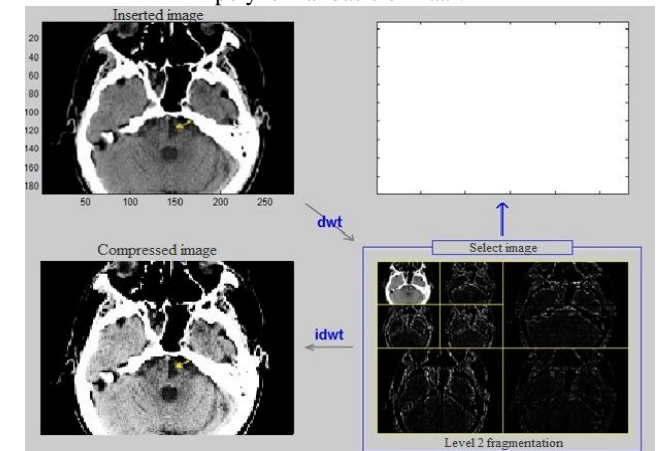


Figure 6: Level 2 fragmentation in two-dimensional piecewise- polynomial basis of Haar

Coefficients of recovery after 1st degree fragmentation as a result of digital processing of X-ray image of the head (Table 1)[12].

Table 1: Coefficients of Recovery after 1st Degree fragmentation

№-odd numbers	$\alpha_j(s)$ - Image recovery coefficients (OQ)	№-couple numbers	$\beta_j(s)$ - Image recovery coefficients (FQ)
1.	0	2.	0
3.	0	4.	0
5.	0	6.	0
7.	509	8.	507,5
9.	507,5	10.	492,5
11.	307	12.	187
13.	0	14.	0
15.	437,25	16.	479,75
17.	493,75	18.	536,25
19.	669,5	20.	824,75
21.	976	22.	212,5
23.	700	24.	720,75
25.	1016	26.	1006,25

Coefficients of recovery after 2nd degree fragmentation as a result of digital processing of the radiographic image of the head (Table 2)

Table 2: Coefficients of recovery after 2nd degree fragmentations

№-odd numbers	$\alpha_j(s)$ - Image recovery coefficients (OQ)	№- couple numbers	$\beta_j(s)$ - Image recovery coefficients (FQ)
1.	0	2.	0
3.	0	4.	0
5.	0	6.	0
7.	277,5	8.	225,5
9.	229	10.	102
11.	109	12.	507
13.	0	14.	0
15.	524,25	16.	533
17.	489,75	18.	457,75
19.	614,75	20.	639,5
21.	690	22.	971,5
23.	1016	24.	1020
25.	4,75	26.	24,25

5. CONCLUSION

With the help of two-dimensional fragment-polynomial basis as a result of digital image processing, an algorithm has been developed that 1-level and 2-level compression of images, based on improving the quality of the compressed

image and determining its recovery coefficients.

As a result, the compressed image is made brighter than the existing image. The amount of these coefficients is 159 048 after the 1st degree decomposition, after 2nd level fragmentation, it was 159 330. The large amount of these coefficients gives more positive results in image recovery. This developed algorithm can also be widely used in determining the number of spots in a subsequent image.

REFERENCES

1. Filtration of signals and images: Fourier and wavelet algorithms (with examples in Mathcad): monograph / Yu. E. Voskoboinikov, A. V. Gochakov, A. B. Kolker; Novosib. state architecture.-builds. un-t (Sibstrin). - Novosibirsk: NGASU (Sibstrin), 2010. -- 188 p.
2. Hidayov, O., Ukaegbu, I. A., Zaynidinov, H., & Lee, S. G. (2010). Comparative analysis of piecewise-polynomial of local basis. In International Conference on Advanced Communication Technology, ICACT (Vol. 2, pp. 947–950).
3. Singh, D., Singh, M., & Hakimjon, Z. (2019). Requirements of MATLAB/Simulink for signals. In SpringerBriefs in Applied Sciences and Technology (pp. 47–54). Springer Verlag. https://doi.org/10.1007/978-981-13-2239-6_6
4. S. Welstead. Fractals and wavelets for image compression in action. // Textbook. - M.: Publishing House Triums, 2003. – 320p.
5. Svinin S.F. Baseline splines in signal theory. SP: Science. 2003. 118p
6. Blatter K. Wavelet analysis. Fundamentals of theory. M.: Technosphere. 2006. 272 p.
7. Singh, D., Singh, M., & Hakimjon, Z. (2019). Requirements of MATLAB/Simulink for signals. In Springer Briefs in Applied Sciences and Technology (pp. 47–54). Springer Verlag. https://doi.org/10.1007/978-981-13-2239-6_6
8. Singh, D., Zaynidinov, H., & Lee, H. J. (2010). Piecewise-quadratic Harmut basis functions and their application to problems in digital signal processing. International Journal of Communication Systems, 23(6–7), 751–762. <https://doi.org/10.1002/dac.1093>
9. Smolentsev N.K. Fundamentals theory of wavelets. Wavelets in Matlab. - M.: DMK Press, 2005. -- 304p.
10. Smolentsev N.K. Fundamentals theory of wavelets. Wavelets in Matlab. - M.: DMK Press, 2005. -- 304p.
11. Stark G. G. The use of wavelets for DSP. - M.: Techno sphere, 2007. -- 192 p.
12. Yakovlev A.N. Introduction to wavelet transforms. -Novosibirsk: NSTU, 2003. -- 104 p.
13. Modern Sampling Theory: Mathematics and Applications. Benedetto J., Ferreiro P. // Springer Science and Business Media LLC. 2012. 158p.
14. Zaynidinov, H., Zaynutdinova, M., & Nazirova, E. (2018). Digital processing of two-dimensional signals in

the basis of Haar wavelets. In ACM International Conference Proceeding Series (pp. 130–133). Association for Computing Machinery. <https://doi.org/10.1145/3274005.3274023>

15. Zaynidinov, H. N., & Mallayev, O. U. (2019). Paralleling of calculations and vectorization of processes in digital treatment of seismic signals by cubic spline. In IOP Conference Series: Materials Science and Engineering (Vol. 537). Institute of Physics Publishing. <https://doi.org/10.1088/1757-899X/537/3/032002>